

INTRODUCTION

Proton resonance frequency shift (PRFS) thermometry¹ is the current standard for MR-based temperature monitoring in interventional procedures. However, PRFS thermometry suffers several limitations, including decreased precision with increased heating due to changes in T_1 and T_2 with heat, and sensitivity to spurious artifacts such as the motion of water in transcranial focused ultrasound².

Since quadratic RF phase MR fingerprinting (qRF-MRF) can quantify off-resonance using much shorter TEs than GRE scans³, it can be used to convert the mapped off-resonance to temperature with less sensitivity to motion⁴. Measuring off-resonance, T_1 , and T_2 simultaneously requires long dynamic scan times, so we propose to map temperature primarily from PRF shift, with a frame rate of 3 seconds or less. Here we describe a constant-flip-angle, short-TE qRF-MRF sequence for MR thermometry.

MECHANISM SIMULATION

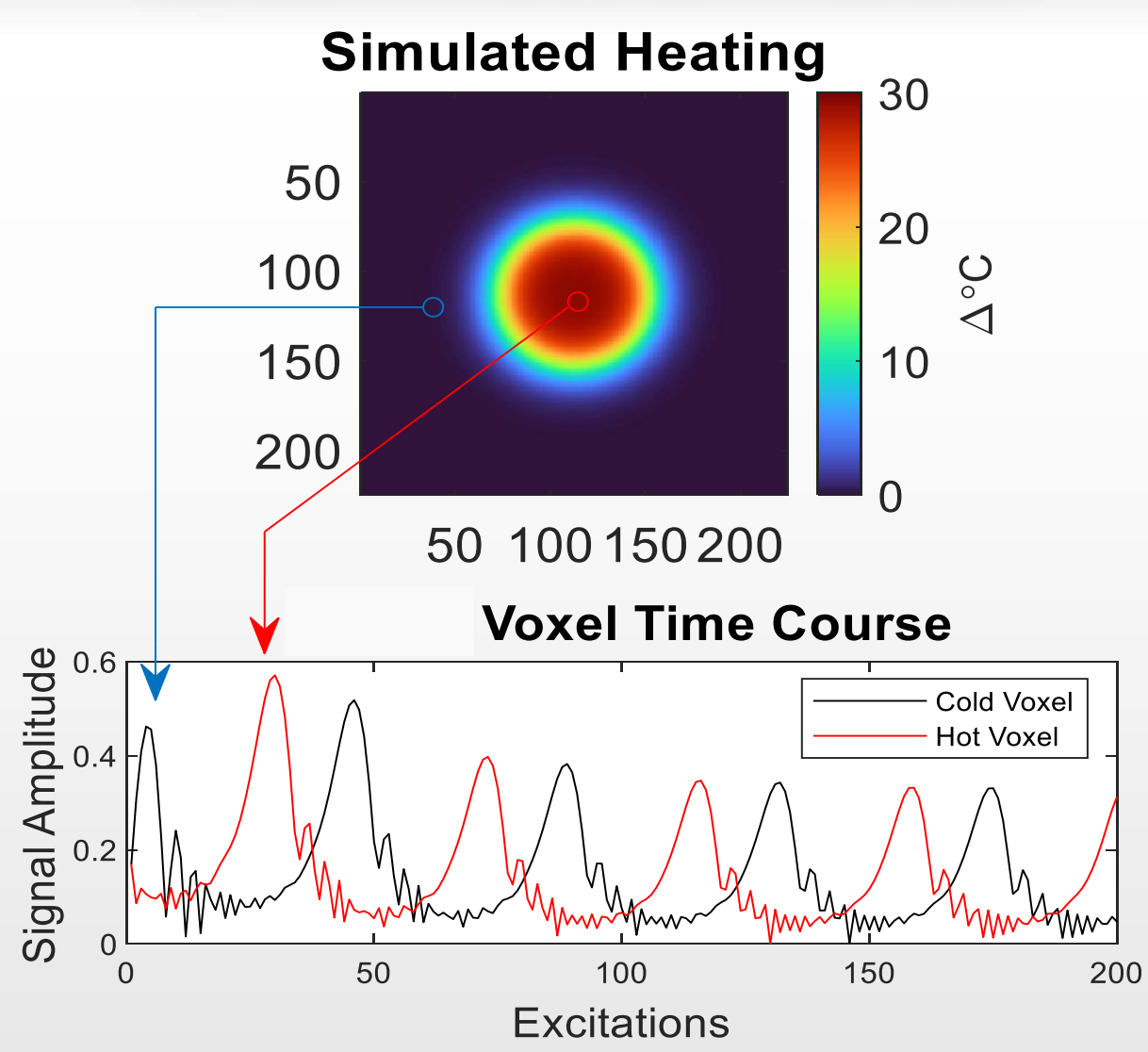


Figure 1. How qRF-MRF thermometry works: The RF quadratic phase corresponds to a repeating frequency sweep, and as the sequence sweeps past each resonance frequency, magnetization at that frequency is coherently excited and its signal increases in amplitude for several TRs, then decays again as the sequence's frequency shifts away. This means that a heated (off-resonant) voxel will refocus at a different time than an unheated (on-resonant) voxel, and overall have a different time course, enabling a dictionary match for temperature.

PHANTOM METHODS

Phantom Setup:

- 3T (Elition X, Philips Healthcare), 32-channel Rx
- qRF-MRF sequence & Dictionary:
 - Quadratic RF phase = $4.2n^2$ radians ($n = \text{TR index}$)
 - Constant TR = 15.5 ms, TE = 2.2 ms, FA = 10°
 - $1.72 \times 1.72 \times 4 \text{ mm}^3$ resolution
 - 250 TRs/3.9 s per dynamic by default
 - Dictionary: $T_1 = 2000 \text{ ms}$, 21 T_2 values (10 to 200 ms), 4 initial M_z values (0.4, 0.5, 0.6, 1), 1024 temperature values (-10 to 40°C)
- Comparison GRE-EPI (5 echoes per TR) sequence
 - 12 ms TE, 5 slices, 130 ms TR, 20° flip angle
 - $0.43 \times 0.54 \times 5 \text{ mm}^3$ resolution
 - 5.3 sec/image dynamic scan time
- $110 \times 110 \text{ mm}^2$ FOV for both.

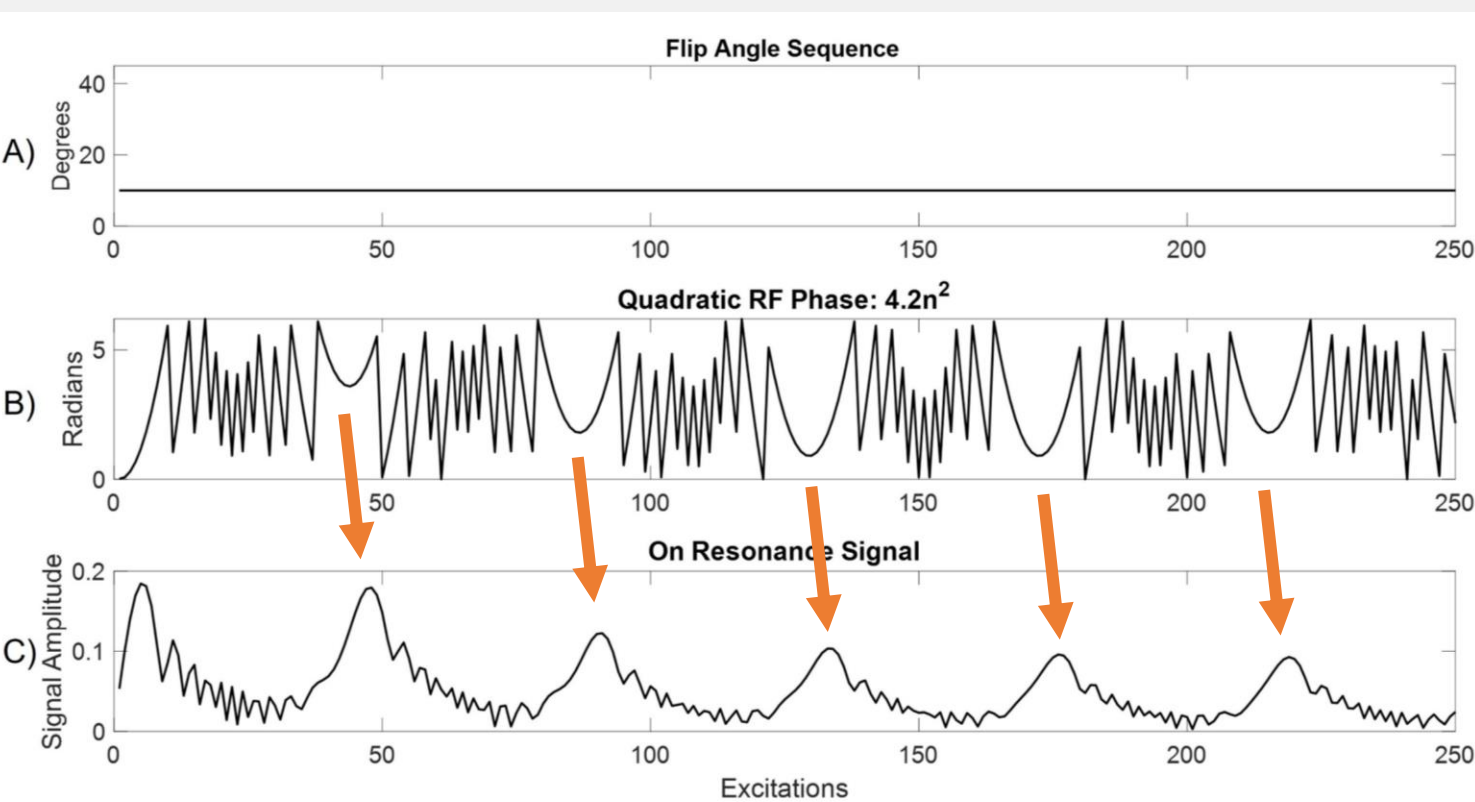


Figure 2. The qRF-MRF sequence uses (a) a constant flip angle of 10° and (b) quadratic RF phase. (c) The signal time course of on-resonance magnetization. Signal peaks occur just after the phase smooths out, when the sequence's instantaneous frequency passes through resonance (arrows).

LASER HEATING EXPERIMENT

- Rectangular phantom comprising 1% agar by volume of water.
- Class 3b BWTek BWF5-980-15 ablation laser (Plainsboro, NJ, USA).
- 3W continuous-wave mode using a 400 micron optical fiber.
- Images acquired as transverse slices perpendicular to the optical fiber.

PHANTOM RESULTS

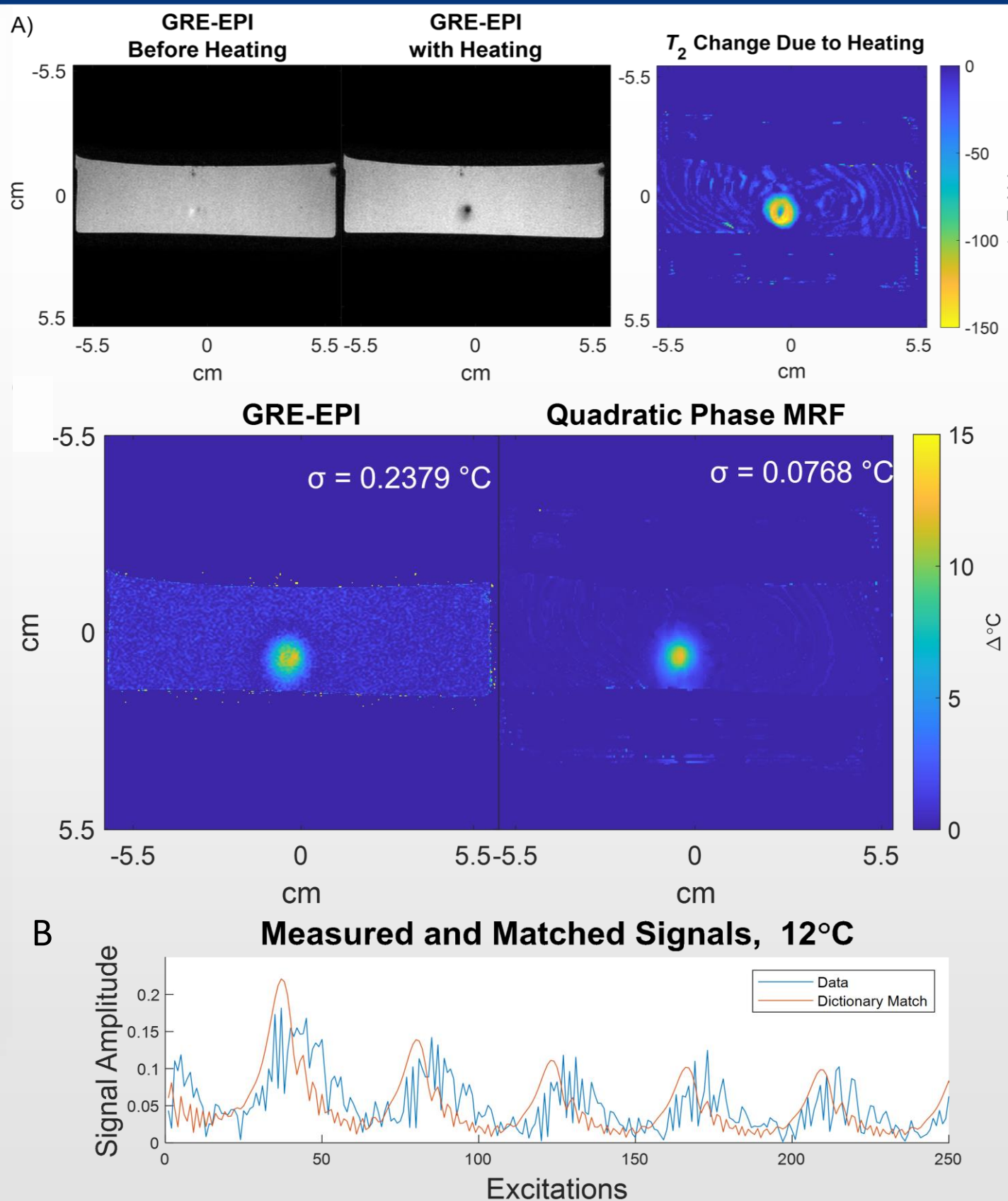


Figure 3. a) Temperature map from the GRE-EPI PRFS method shown next to a qRF-MRF map. Background temperature precision was $\sim 3\times$ higher in the qRF-MRF temperature map. b) The signal time course of the center hot spot voxel in the qRF-MRF map along with its corresponding dictionary match.

IN VIVO METHODS

In Vivo Setup:

- 3T (Vida, Siemens Healthcare), 16-channel Rx
- Constant 10° flip angle, TR = 10 ms, TE = 2.5 ms
- Quadratic excitation pulse RF phase of $4.2n^2$ radians for $n = 300$ TRs for sensitivity to off-resonance.
- Comparison 2DFT sequence: TE = 12 ms, TR = 17 ms (2.2 s per dynamic)
- Both sequences: $256 \times 256 \text{ mm}^2$ FOV, axial slice, $2 \times 2 \times 5 \text{ mm}^3$ resolution
- Dictionary: (-50,50) Hz with 2048 points and 21 linewidths, $T_1 = 825 \text{ ms}$, $T_2 = 70 \text{ ms}$ (average grey/white matter), convolved with 21 linewidths to account for intravoxel dephasing

ITERATIVE RECONSTRUCTION



Figure 4. Forward model of the dictionary constrained reconstruction

The dictionary was compressed in SVD space and used to constrain the data. The data were then gridded and reconstructed with 10 iterations of conjugate gradient descent. The resulting images were then matched back to the dictionary as standard MRF processing.

IN VIVO DYNAMIC PROCESSING

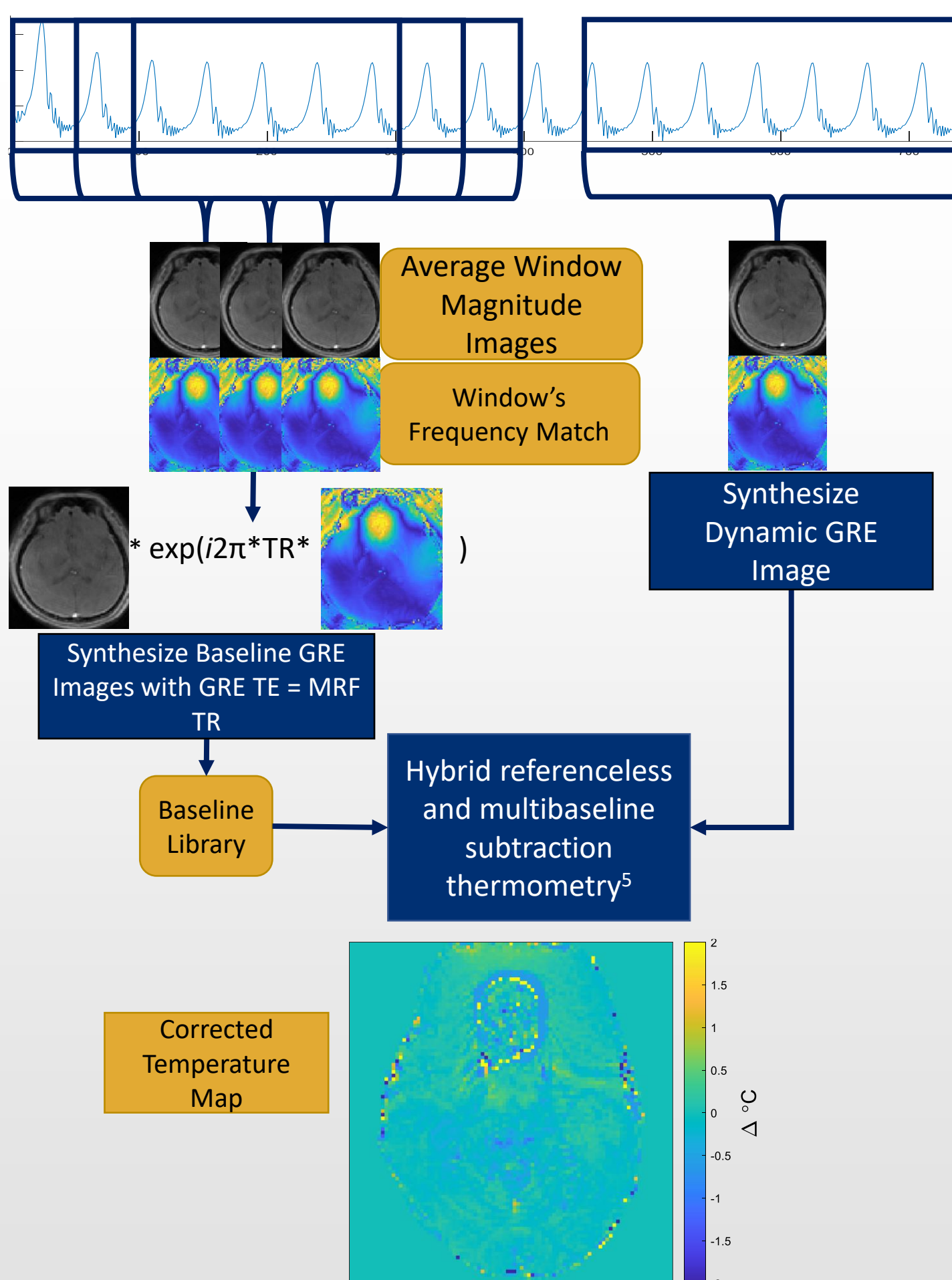


Figure 5. Model of processing from frequency maps and magnitude images to temperature maps.

IN VIVO RESULTS

- Sliding window processing of MRF data allows the qRF-MRF temperature maps to be updated every 0.5 seconds, versus every ~ 2.2 seconds for 2DFT standard method
- 6.5 seconds of baseline scan time = 3 baseline images for 2DFT but 7 baseline images for MRF
- 2nd order referenceless polynomial correction

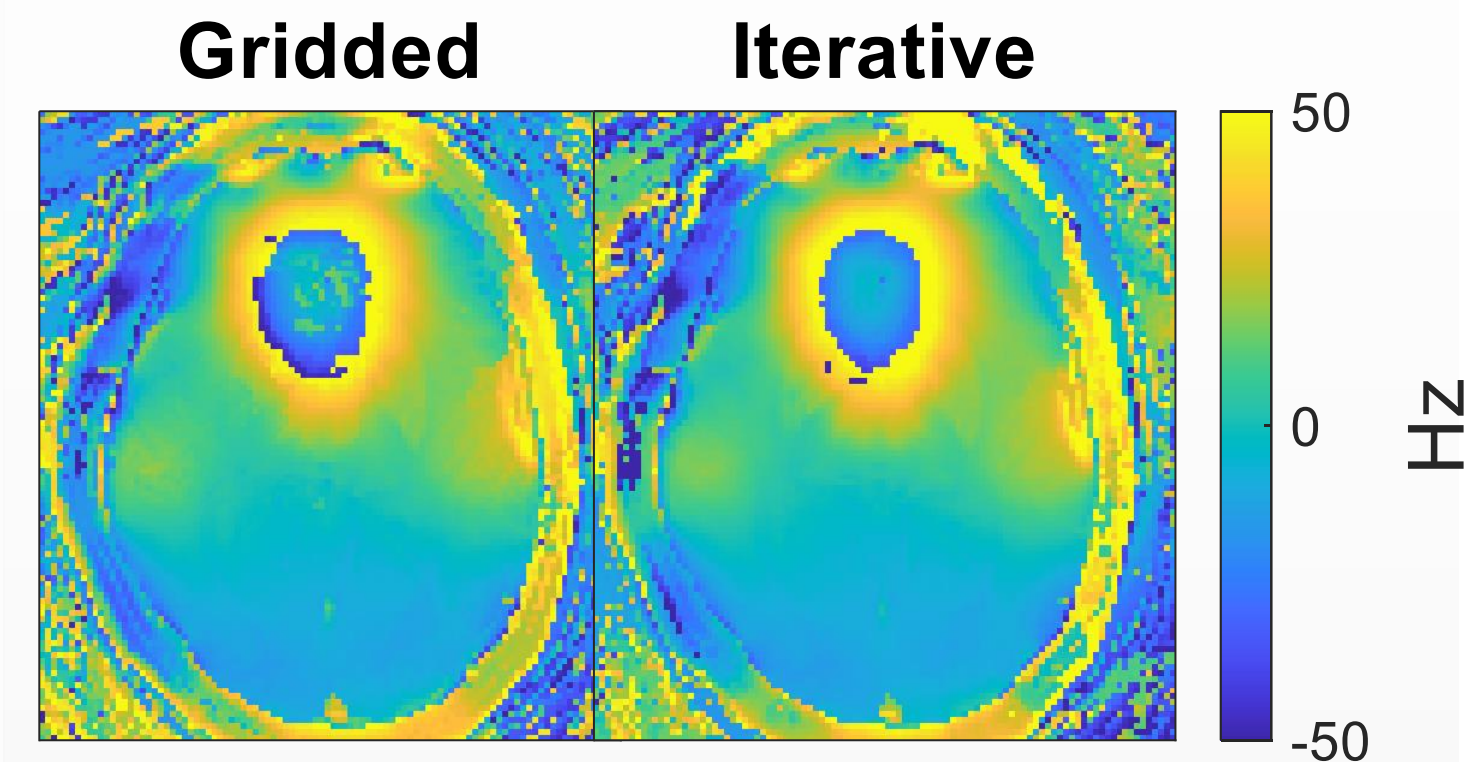


Figure 6. One timepoint of a frequency match in qRF-MRF. The left side shows the frequency match from a gridded image, and the right side shows the same timepoint using the iterative reconstruction method.

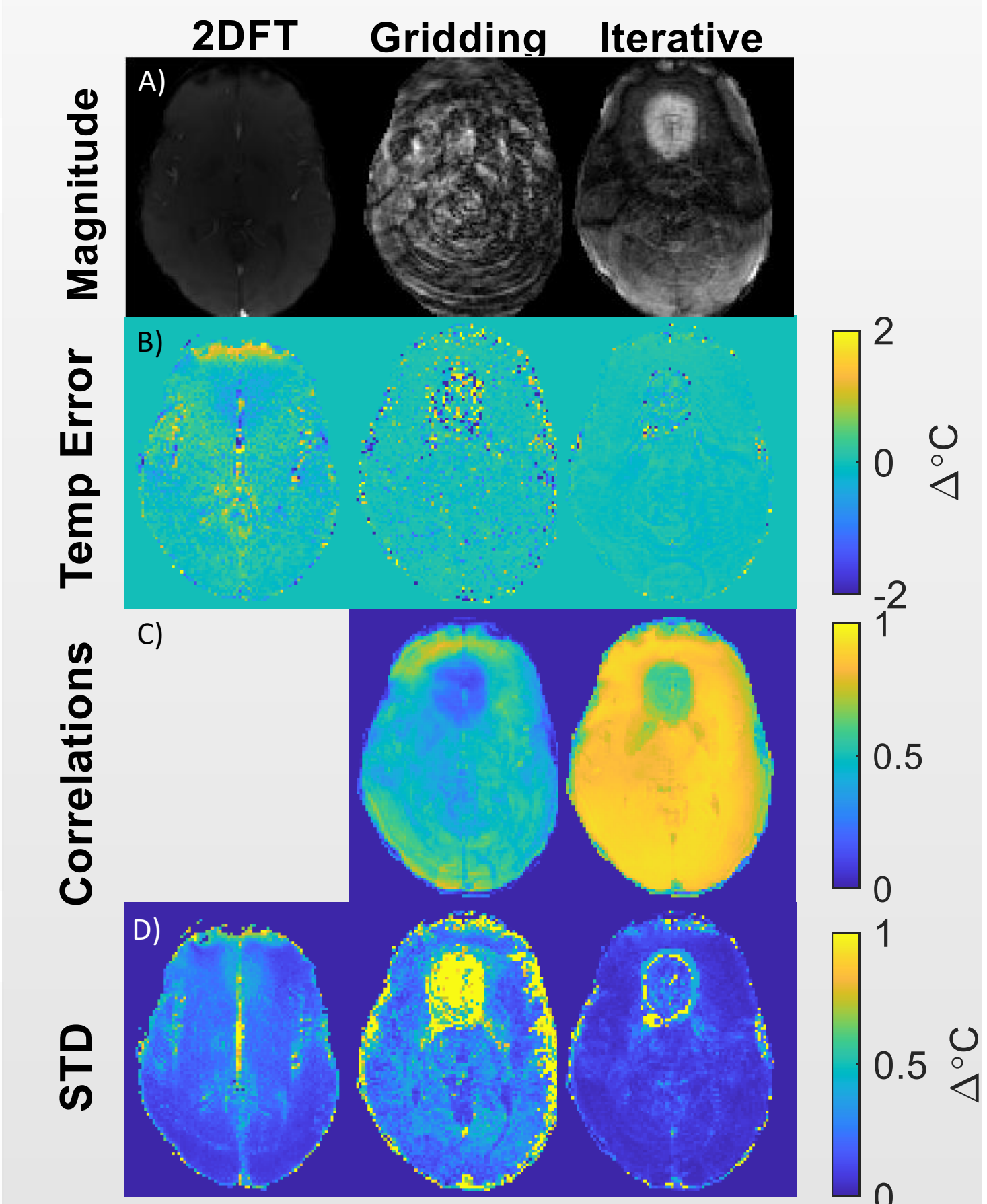


Figure 7. A) Comparison of a single timepoint image in 2DFT, gridded qRF-MRF, and iterative qRF-MRF. B) Temperature error of a single dynamic in a no-heating in vivo scan compared across the three methods. C) The correlations, a measure of the strength of the match, for the two qRF-MRF reconstructions. D) The standard deviation over time in the three cases in the same no-heating in vivo scan.

- Correlations are higher as expected in the constrained iterative reconstruction
- Overall standard deviation is lower in the iterative reconstruction compared to the gridded reconstruction, especially in the area of high susceptibility near the front of the brain

FUTURE WORK

- Address the artifacts at the front of the brain that lead to wrapping and artificial hard edges in the frequency maps
 - Slice profile correction
 - Dictionary adjustments
- Collect data from ultrasound heating

CONCLUSION

Results showed that qRF-MRF temperature mapping can provide precise temperature imaging while simultaneously generating maps of T_2 changes. The method's short TE and repeated sampling of the center of k-space every TR retains signal as T_2 shortens with heating, unlike conventional PRFS scans which use long TEs for high temperature phase contrast and suffer loss of temperature precision with heating.

REFERENCES

- [1] V. Rieke and K. Butts Pauly, *JMRI*, 2008;27:376–390.
- [2] Luo H, et al., *MRM*. 2022;88:2419-2431.
- [3] C. Y. Wang, et al., *MRM*, 2019;81:1849-1862.
- [4] R. Boyacioglu, et al., *Proc. ISMRM*. 2020;28.
- [5] W. Grissom et al., *Med. Phys.* 2010;37(9):5014-5026.

ACKNOWLEDGEMENTS

This work was supported by NIH grants R01 NS120518 and R01 EB028773.